Quantitative Drug Dynamics Visualized by Alkyne-Tagged Plasmonic-Enhanced Raman Microscopy

*Kota Koike[§#†], Kazuki Bando[§†], Jun Ando[§], Hiroyuki Yamakoshi[$], Naoki Terayama[⊥], Kosuke Dodo[⊥], Nicholas Isaac Smith[&], Mikiko Sodeoka[⊥], and Katsumasa Fujita[§#¶] **

AUTHOR ADDRESS

[§]Department of Applied Physics, Osaka University, 2-1 Yamadaoka, Suita, Osaka 565-0871, Japan.

[#]AIST-Osaka University Advanced Photonics and Biosensing Open Innovation Laboratory, National Institute of Advanced Industrial Science and Technology (AIST), 2-1 Yamadaoka, Suita, Osaka 565-0871, Japan.

[$]Graduate School of Pharmaceutical Sciences, Nagoya City University, 3-1 Tanabe-dori, Mizuho-ku, Nagoya, Aichi 467-8603, Japan.

[⊥]Synthetic Organic Chemistry Laboratory, RIKEN Cluster for Pioneering Research, 2-1 Hirosawa, Wako, Saitama 351-0198, Japan.

[&]Immunology Frontier Research Center, Osaka University, 2-1 Yamadaoka, Suita, Osaka 565-0871, Japan.

[¶]Transdimensional Life Imaging Division, Institute for Open and Transdisciplinary Research Initiatives, Osaka University, 2-1 Yamadaoka, Suita, Osaka 565-0871, Japan.

*E-mail: fujita@ap.eng.osaka-u.ac.jp

ABSTRACT

Visualizing live-cell uptake of small molecule drugs is paramount for drug development and pharmaceutical sciences. Bioorthogonal imaging with click chemistry has made significant contributions to the field, visualizing small molecules in cells. Furthermore, recent developments in Raman microscopy, including stimulated Raman scattering (SRS) microscopy, have realized direct visualization of alkyne-tagged small molecule drugs in live cells. However, Raman and SRS microscopy still suffer from limited detection sensitivity with low concentration molecules for observing temporal dynamics of drug uptake. Here, we demonstrate the combination of alkyne-tag and surface-enhanced Raman scattering (SERS) microscopy for the real-time monitoring of drug uptake in live cells. Gold nanoparticles are introduced into lysosomes of live cells by endocytosis, and work as SERS probe. Raman signals of alkyne can be boosted by enhanced electric fields generated by plasmon resonance of gold nanoparticles when alkyne-tagged small molecules are co-localized with the nanoparticles. With time-lapse 3D SERS imaging, this technique allows us to investigate drug uptake by live cells with different chemical and physical conditions. We also perform quantitative evaluation of the uptake speed at the single-cell level using digital SERS counting under different quantities of drug molecules and temperature conditions. Our results illustrate that alkyne-tag SERS microscopy has a potential to be an alternative bioorthogonal imaging technique to investigate temporal dynamics of small molecule uptake of live cells for pharmaceutical research.

KEYWORDS: Raman microscopy, surface-enhanced Raman scattering, gold nanoparticle, drug imaging, small molecule

Raman microscopy enables us to visualize molecular distributions without labeling and is utilized in biological fields, which require noninvasive detection. Live-cell Raman imaging with various types of cellular dynamics has been performed.[1-4] In cells, however, Raman peaks of molecules of interest usually appear in the Raman "fingerprint" region, where numerous endogenous molecules show Raman peaks. It is therefore often difficult to selectively detect Raman signal from specific molecules. An application currently lacking in techniques for visualizing specific molecules and their uptake dynamics in a cell is the imaging of intracellular small molecule drug dynamics. In this type of imaging, the identification of the drug molecules locations in the cells, and the distinction of these molecules from endogenous intracellular molecules are required. This type of information allows us to optimize the design of drug molecules to improve the uptake rates and/or medical efficacies, especially when the temporal resolution is high enough to track the uptake and intracellular dynamics.[5,6] However, the complex intracellular environment makes it difficult to observe the drug itself, especially at physiological concentrations. To identify these Raman signals amongst the large background of intracellular molecules, the use of alkyne as a tiny and specific Raman-tag has been proposed.[7,8]

Alkynes are almost unique in that they have small structures, do not originally present inside of live cells, and are bioorthogonal. With these features, click chemistry with azide–alkyne cycloadditions can be applied to bioorthogonal imaging of nearly any biological small molecules and has provided tremendous progresses in understanding biological processes involved with small molecules.[9,10] However, relatively bulky fluorophores, attached to alkyne- or azide-tagged small molecules through click reactions, may alter functional properties of small molecules and also cause photo-bleaching. These issues can limit the application of click chemistry with fluorescence techniques for the study of temporal dynamics of drug uptake (needing repeated exposures over

time) in live cells. Alkynes are also spectroscopically bioorthogonal, exhibiting a Raman peak at around 2120 cm^{-1}, which is in the silent wavenumber region, where endogenous molecules do not usually exhibit Raman peaks. This characteristic allows us to directly visualize alkyne-tagged small molecules using Raman microscopy.[7,8,11-13] Stimulated Raman scattering (SRS) microscopy, which boosts the imaging time and molecular specificity through coherent oscillations of specific molecular vibrations, is an emerging tool for visualizing the spatial distribution of small molecule drug. [14-18] However, detection limits of molecules with SRS microscopy are typically at the mM level, which is similar to that with spontaneous Raman microscopy. It is therefore challenging with SRS microscopy to visualize the temporal dynamics of early time stages of drug uptake, where local concentrations of small molecules are below the detection limits.

Here, we propose the use of surface-enhanced Raman scattering (SERS) to increase the detection sensitivity by plasmon resonance in metallic nanoparticles, and thereby detect alkyne-tagged small molecule drugs in live cells, while maintaining full 3-dimensionally (3D) imaging capability with temporal resolution high enough to track the drug distribution as it is taken up by the cell. SERS spectroscopy has been used to detect molecules at low concentrations *via* signal enhancement by localized plasmon resonance in metal nanoparticles.[19–22] While SERS has offered strong potential to improve the detection sensitivity and temporal resolution in live-cell imaging,[23,24] the fluctuations of both signal intensity and peak position, which are due to high sensitivity to the interaction between molecules and the metal surface, have hindered practical use of SERS in biomedical applications.[25,26] In addition, SERS peaks of small molecules may also overlap with that of endogenous molecules at the Raman fingerprint region. However, the combination of SERS and alkyne-tag can solve this issue since the unique alkyne signal can be detected separately from Raman peaks from endogenous molecules.[27-30] In our technique, gold

nanoparticles introduced in live cells work as agents to report the arrival of alkyne-tagged small molecule drugs at lysosomes, where the nanoparticles also localize during the transport.[23-26,31] Terminal alkynes show a high affinity to the surface of metals, such as silver and gold.[27-30,32,33] Therefore, strong enhancement of the Raman signal from alkyne can be expected due to chemical adsorption onto the surface of nanoparticles. We utilized an alkyne-tagged acyloxymethyl ketone type inhibitor (Alt-AOMK),[33] an alkyne-tagged cathepsin B inhibitor, as a small molecule drug. 3D SERS imaging was performed with home-built slit-scattering Raman microscopy, which achieves temporal resolution high enough to visualize drug uptake with the enhancement of the Raman signal. We also propose the use of a 3D voxel-counting digital SERS technique in order to cancel the fluctuations of the signal intensity and provide quantitative analysis of drug uptake over time. The number of voxels where the target drug exists are counted, and the concentration-dependent uptake process can then be visualized by the time-resolved 3D SERS datasets. Our findings show SERS technique can boost the detection sensitivity of small molecules drugs in live cells and thus has strong potential to be an alternative way of bioorthogonal small molecule imaging currently led by click-chemistry and stimulated Raman microscopy.

RESULTS AND DISCUSSION

We used Alt-AOMK designed from Z-FG-AOMK as a small molecule drug in our experiment (Figure 1A). Z-FG-AOMK was developed as a selective inhibitor of the lysosomal cysteine protease cathepsin B (CatB) localized in lysosomes.[34] The efficacy of Alt-AMOK as a CatB inhibitor was also confirmed in our previous study[33] while its uptake processes and dynamics within cells have remained unknown. The alkyne peak of Alt-AOMK was observed at 2122 cm^{-1}

in the spontaneous Raman spectrum (Figure 1B). Other Raman peaks at 1176 cm^{-1} and 1613 cm^{-1} can be assigned to vibrational modes of aromatic C-H bending and ring stretching, respectively.[35] The other peaks at 1040 cm^{-1}, 1320 cm^{-1}, and 1418 cm^{-1} are derived from dimethyl sulfoxide (DMSO) used as the solvent. We also confirmed that the detection limit of the alkyne peak of Alt-AOMK was approximately 4 mM with spontaneous Raman scattering (Figure S1). We then measured the SERS spectrum of Alt-AOMK dropped on a gold nanoparticles-modified glass substrate. The SERS peak of alkyne at approximately 1980 cm^{-1} was confirmed with SNR of 11.4 at a concentration of 10 μM (Figure 1B), which is beyond the detection limit of spontaneous Raman spectroscopy. The other peaks at approximately 1163 cm^{-1} and 1594 cm^{-1} can be assigned to the enhanced Raman signal of aromatic-ring vibrational modes of Alt-AOMK. The blue-shift of the alkyne peak with approximately 140 cm^{-1} was mainly caused by the electron donation from alkyne to the gold nanoparticles through coordination of alkyne onto the surface of the nanoparticles, and the spectral broadening of the peak can be explained by the existence of several molecular orientations adsorbed onto the surface.[35-38] Since the alkyne peak locates in the Raman silent region, it can be used for selective detection of Alt-AOMK in live cells without interference with endogenous molecules by Raman microscopy.

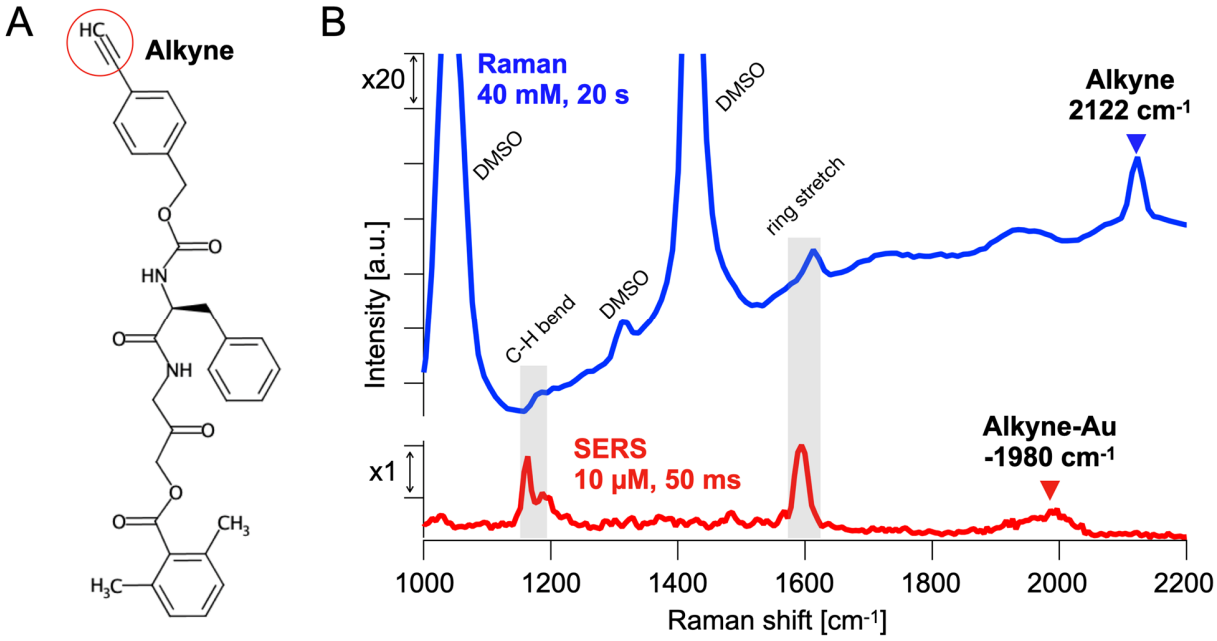

Figure 1. Raman spectroscopy of alkyne-tagged acyloxymethyl ketone type inhibitor (Alt-AOMK). (A) Molecular structure of Alt-AOMK. (B) Raman spectrum (blue color) of Alt-AOMK at a concentration of 40 mM and surface-enhanced Raman scattering (SERS) spectrum (red color) of Alt-AOMK at a concentration of 10 µM. The excitation intensities and exposure times were 2 mW/µm^2 and 20 s for the spontaneous Raman measurement, and 0.79 mW/µm^2 and 50 ms for the SERS measurement.

Macrophages J774A.1 were used for the live-cell SERS imaging. Previous studies using macrophages successfully demonstrated live-cell SERS measurements with gold nanoparticles in lysosomes.[24-26] Also, overexpression of CatB, which is a target of Alt-AOMK and locates in lysosomes, in macrophages has been studied for metabolic diseases.[39,40] Macrophages are also of particular interest for Alt-AOMK studies, since inhibition\ of CatB reduces their ability to produce TNF- α, a potent cytokine which is fundamental to the main immunological role of macrophages.[41] We used a home-built slit-scanning Raman microscope[3,4,42] equipped with a 660 nm laser as the excitation source (see Figure S2 for details of the optical setup). After culturing the macrophages with and without gold nanoparticles for 16 h, Alt-AOMK was introduced into the culturing medium at a final concentration of 10 µM. Raman images of these samples showed the

enhancement of SERS signals from both endogenous molecules and alkyne in the cells with gold nanoparticles (Figure S3), which confirms the sensitivity improvement in molecular detection by using SERS. We also confirmed gold nanoparticles and Alt-AOMK have low toxicity for live cells based on cell viability assay (Figure S4, Table S1).

To monitor the drug uptake into live cells, along with sensitivity, temporal resolution that is adequate for tracking the dynamics of small molecule drugs is also required. The signal enhancement in SERS facilitates the possibility of high-speed molecular imaging. We demonstrated time-lapse SERS imaging of macrophages to visualize the spatiotemporal dynamics of Alt-AOMK (Figure 2A, Supporting Movie 1). SERS images with an area of 80 × 173 μm were obtained with an image acquisition rate of 6.5 s. Image acquisition was continuously performed at the same area for 43 min (Figure 2A). The temporal change of the distribution of SERS signals from alkyne indicates the movement of Alt-AOMK and/or gold nanoparticles inside the cells. Blurred SERS signals were given from the particles at out-of-focal planes. SERS spectra obtained from the selected single pixels (Figure 2B) exhibited the alkyne peaks (Figure 2C). The alkyne peak position differed slightly depending on the positions of the SERS signals, suggesting differences in the orientation of Alt-AOMK inside the SERS hotspots and the distance between Alt-AOMK and the metal surface. Such peak fluctuations of the SERS spectrum have been observed previously with analytes under low concentration conditions.[43,44] Based on the SERS spectrum of Alt-AOMK (Figure 1B), SERS peaks around 1160 cm^{-1} and 1580 cm^{-1} can be assigned to Alt-AOMK. Several SERS peaks between 1160 cm^{-1} and 1580 cm^{-1}, which are not assigned to the SERS peaks of Alt-AOMK, were also detected, indicating the co-existence with endogenous molecules at the same hotspot. In the images of the cells without Alt-AOMK, no SERS signal was observed in the silent region; however, endogenous molecules showed SERS signals in the

fingerprint region (Supporting Movie 2). Figure 2D shows a time series of SERS images of the single cell surrounded by the black dotted-square in Figure 2A. The SERS spectra obtained from one of the bright spots (Figure 2E) showed the fluctuations of intensity and peak positions of the SERS signal from alkyne. This result indicates temporal variations in the interaction between Alt-AOMK and the gold surface during the observation period, such as changes in the adsorbed distance and orientation. SERS signals from adsorbed molecules have shown such temporal variations.[45] By performing 3D SERS imaging of live macrophages, we confirmed that Alt-AOMK generating SERS signals were inside the cells (Figure S5), as expected, rather than originating from the substrate or other out-of-cell locations.

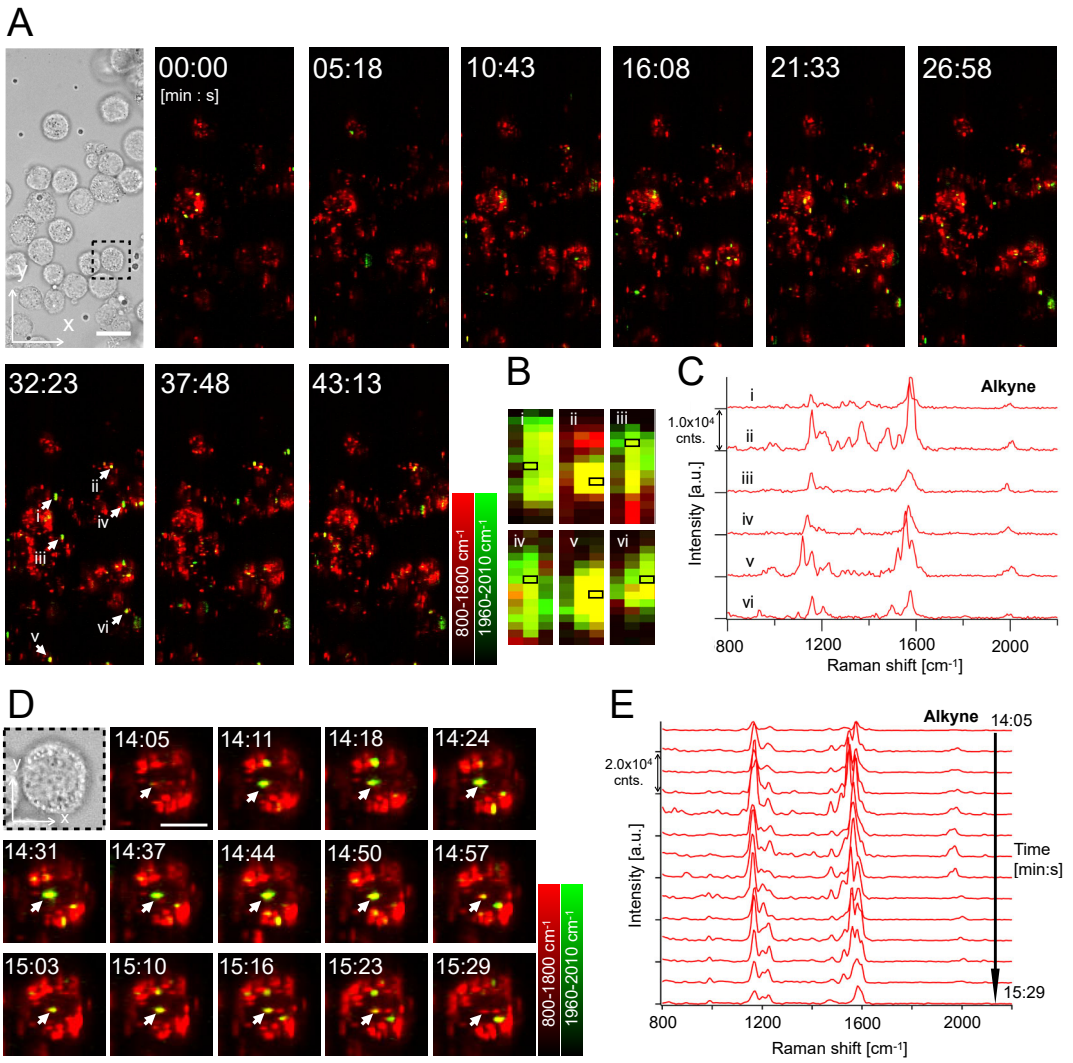

Figure 2. Time-lapse 2D SERS imaging of living macrophages with Alt-AOMK. (A) Bright field and SERS images of the cells. The SERS images were reconstructed from two Raman spectral windows; the red color is the average Raman intensity from 800 to 1800 cm^{-1} containing Raman peaks of endogenous molecules, and the green color is the average Raman intensity from 1960 to 2010 cm^{-1} assigned to the alkyne peak. Scale bar = 20 μm. (B) Magnified SERS signals of alkyne indicated as the white arrows in (A) at the time point 32 min 23 s. (C) SERS spectra from each single pixel indicated by the black squares in (B). Only background subtraction was applied for spectral processing. (D) Time-lapse SERS images of the single cell in (A). Scale bar = 10 μm. (E) Time series of the SERS spectra obtained from the SERS signals indicated by white arrows in (D).

To observe the process of drug uptake, 3D imaging of cellular volumes is useful to validate how small molecule drugs can distribute inside the entire cell body as we showed in Figure S5.

We performed time-lapse 3D SERS imaging to monitor the drug uptake of macrophages (Figure 3 and Supporting Movie 3). The 3D SERS images were recorded for approximately 53 min with an acquisition time of approximately 22 s per image. Although the image acquisition time for the 3D imaging was longer than that for the 2D imaging, it was still fast enough to observe the uptake of Alt-AOMK. During the measurement (6 min after starting the imaging), we added cell-culturing medium (DMEM) containing Alt-AOMK to the dish to reach a final concentration of Alt-AOMK at 20 μM. SERS signals of alkyne were detected in several cells at approximately 15 min after the drug administration, and was found to gradually increase. There was no obvious morphology change in the cells after the time-lapse 3D SERS imaging for 53 min (Figure S6). The SERS imaging for more than 70 min introduced photodamage in some cells under observation while the other cells did not show significant morphological degradations (Figure S7). Gold nanoparticles can be accumulated into lysosomes with forming nanoparticle clusters with the incubation for 16 h.[46] In addition, the SERS intensity from endogenous molecules (800-1800 cm^{-1}) and its temporal behavoir was almost constant over time (Figure 2A, Figure 3B). Therefore, during the imaging, we can presume there is no significant change in the amounts of the nanoparticles, apart from the always-present stochastic changes due to random motion of the particles, molecular diffusion, and inherent SERS blinking. Based on these considerations, the probability of co-localization of alkyne with gold nanoparticles should increase as the amount of Alt-AOMK incorporated into the cells increases. Thus, the number of SERS spots of alkyne can be correlated with the relative change in the Alt-AOMK concentration in the cells although absolute quantification of the concentration would be highly challenging.

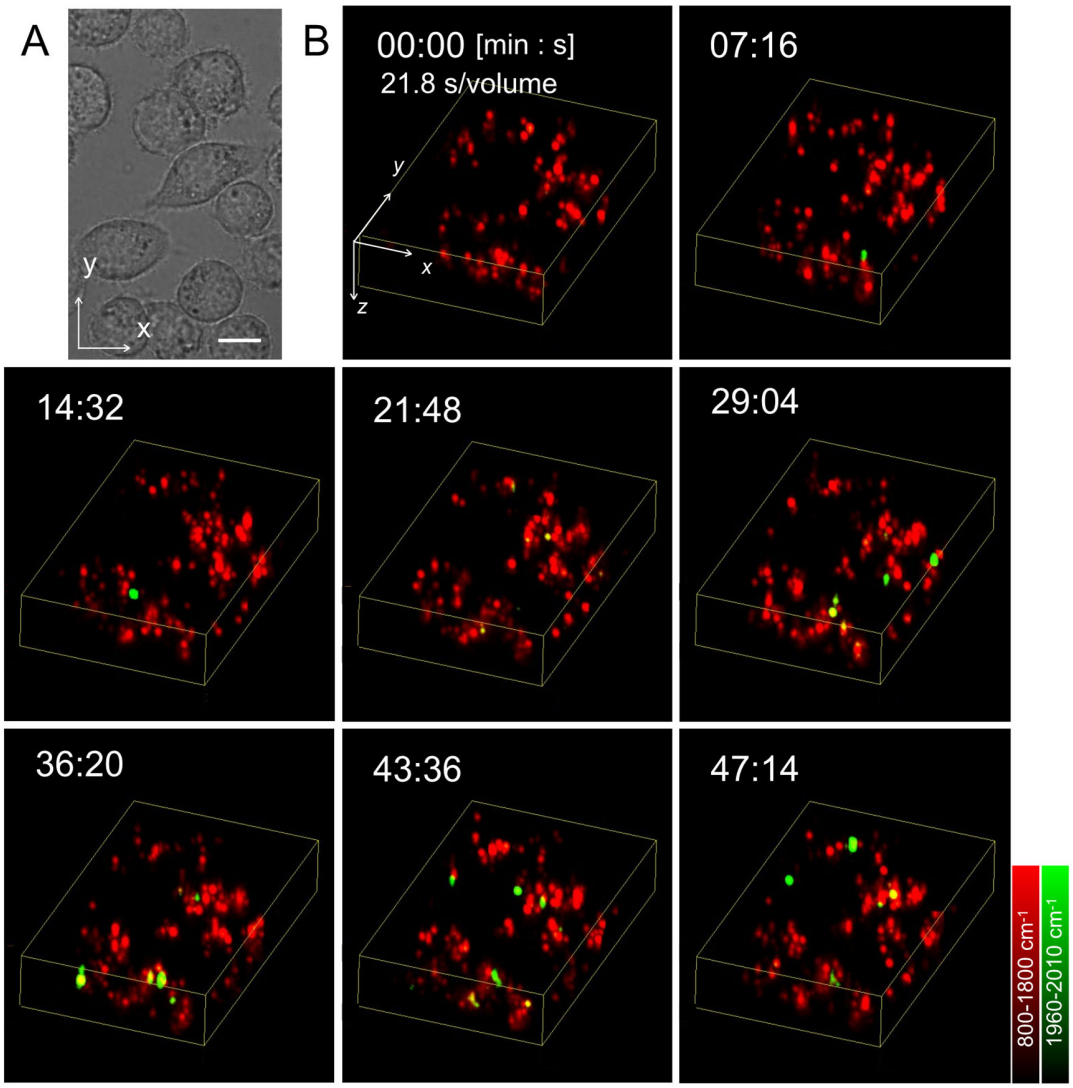

Figure 3. Time-lapse 3D SERS imaging of living macrophages to monitor the uptake of Alt-AOMK into the cells. (A) Bright field image of the cells. Scale bar = 10 μm. (B) Time-lapse 3D SERS images of the cells. Alt-AOMK was introduced into the cell culture dish at a concentration of 20 μM. The SERS images were reconstructed from two Raman spectral windows; the red color is the average Raman intensity from 800 to 1800 cm^{-1}, and the green color is the average Raman intensity from 1960 to 2010 cm^{-1}. Timeline indicates the time after the drug administration. The imaging volume was 50 × 82 × 15 μm.

Recently, the digital SERS counting technique[47] based on the concept of digital bioassays[48] was proposed as a method to quantify the low-concentration analyte. We applied the technique to evaluate the temporal behavior in the number of SERS spots of alkyne in each cell. Briefly, each

voxel of a 3D SERS image was digitized to 1 (with alkyne) or 0 (without alkyne) when the SERS intensity of alkyne was either above or below the threshold value, respectively (Figure 4A, Figure S8). Then, we created a cell-distribution map based on a bright field image and SERS image to count the number of SERS spots of alkyne in each cell (Figure 4B). Finally, we counted the number of SERS spots for all frames (Figure 4A). The number of alkyne-containing voxels differed from cell to cell (Figure S9), which suggests that the uptake reaction or the number of gold nanoparticles differed between the cells. Although the measurement of the absolute drug concentration was not available with this technique, the temporal change of the number of SERS spots reflects the speed of drug uptake. At a concentration of 20 μM, as shown in Figure 3B, the number of SERS spots increased approximately 10–15 min after drug administration, indicating the uptake of Alt-AOMK into the cells occurred during this period. We then measured the concentration dependence on the temporal behaviors of the number of SERS spots (Figure 4C, Supporting Movie 4). We found that the temporal behaviors of SERS spots strongly depended on the concentrations. With increasing administration concentration, the drugs were detected within a shorter time. At 100 μM, the alkyne signals were detected as early as few minutes after the drug administration. We also confirmed a linear relationship between the concentration of Alt-AOMK in the culturing medium and the number of SERS spots at the relatively steady state (47 min after the drug administration) as shown in Figure 4D. The combination of SERS imaging and digital counting quantitatively visualized the temporal behaviors of drug uptake under different chemical concentrations, which have been difficult to perform using conventional techniques. Although it does not currently allow absolute concentration measurement, the linearity of the measurement demonstrates the utility of such uptake time profiles.

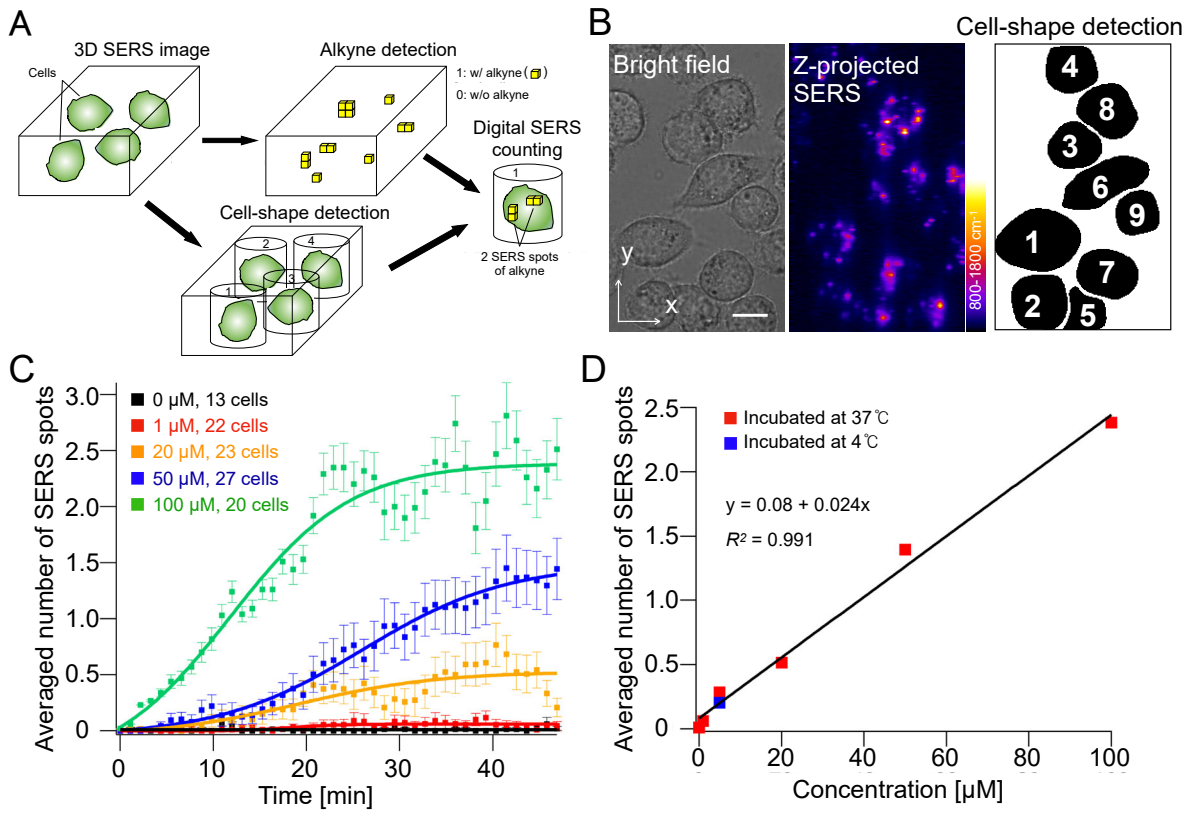

Figure 4. Quantitative detection of SERS spots exhibiting the alkyne peak at around 1980 cm^{-1}. (A) Scheme for counting the number of SERS spots of alkyne in each cell. Each voxel of the SERS image was replaced with 1 if the spectrum had the alkyne signal (see Figure S8 for the detailed protocol). Note that we did not count one independent voxel with the value of 1 with no neighboring voxel of 1. (B) Cell-shape detection of the cells. In this case, nine cells were used for the counting of the SERS spots. Scale bar = 10 μm. (C) Temporal behaviors of the number of SERS spots of alkyne at different concentrations. Squared dots at each color are the temporally averaged number of the SERS spots with a window of 5 frames. Sigmoid fitting was applied to the dots for each concentration except 0 μM. Linear fitting was employed to the dots of 0 μM. Because no drug molecule was applied at 0 μM, the number of SERS spots exhibiting the alkyne peak was mostly zero. The error bar is ±SE (standard error). (D) Relationship between concentrations of Alt-AOMK and maximum values of sigmoid fitting on the temporal behaviors of the number of SERS spots. The values at 0 μM, 1 μM, 20 μM, 50 μM, and 100 μM were obtained from the result shown in (C). The other two values at 5 μM were obtained from the results shown in Figure S11. A linear fitting was performed using all plotted points.

We applied our technique to investigate the temperature dependence on the uptake of Alt-AOMK. Incubating live cells at a low temperature such as 4 °C for hours can effectively block the

endocytosis transport while keeping the cells alive.[49,50] On the other hand, the cellular permeation through the lipid bilayer can still occur by following the concentration gradient of molecules between the inside and outside the cells. Therefore, comparison of the temporal behaviors of SERS spots between the cells incubated at 37 °C and 4 °C was performed for further understanding of the uptake pathway of Alt-AOMK. First, we confirmed that endocytosis of live macrophages was effectively blocked by 4 °C incubation (Figure S10). We then performed time-lapse 3D SERS imaging of drug uptake of the cells incubated at 37 °C and 4 °C (Supporting Movie 5). The gold nanoparticles were introduced *via* endocytosis as previously described at 37 °C before the SERS measurement. The temporal behaviors of the SERS spots under the two different conditions were almost identical (Figure S11), indicating that the speed of drug uptake did not show a strong dependence on the temperature. The number of SERS spots obtained from the cells incubated at 4 °C were well fitted on the linear curve as shown in Figure 4D. Considering these results and the fact that Alt-AOMK and lipid bilayer are both hydrophobic molecules, the cells may uptake Alt-AOMK mainly *via* membrane penetration, not endocytosis transportation.

CONCLUSION

In this work, we proposed a method for observing the drug uptake and dynamics in live cells using SERS signal of alkyne. The use of alkyne-tag allowed us to interpret and extract the Raman signature of target molecules without applying complex spectral analysis techniques. Alkyne-tagged small molecules detected by SERS require several conditions; to be incorporated by the cells, and to be co-localized with aggregations of nanoparticles/SERS hotspots. Therefore, our approach is based on using the nanoparticle distribution which is previously uptaken, to sample the target molecules which are uptaken and diffuse through the cell. Endogenous molecules are also detected. Surface charge and incubation time of gold nanoparticles change the localization

and number of SERS hotspots, which affects the probability of the detection. However, in our measurement, the experiments were performed after incubating live cells with gold nanoparticles for 16 h, so that the amount was not expected to systematically change significantly during the experiments, and the drastic change in the temporal behavior of the SERS intensity from endogenous molecules (800-1800 cm^{-1}) was not observed over the measurement period. This suggests the local conditions related to the particle aggregation and the endogenous molecules did not significantly change. Therefore, we can conclude that that the rise in SERS signals of alkyne is primarily due to the relocation of the drug molecules from outside the cells to inside the cells.

Comparison of the SERS signals and degree of co-localization between different cell types and conditions is difficult. However, we can compare the temporal variation of SERS signals within the same cells during observations. Therefore, we applied time-lapse imaging to investigate the temporal variation of SERS signals in the same cells. We successfully visualized the drug uptake process at early time stages with different concentrations of the drugs through time-lapse 2D and 3D SERS imaging.

The time-lapse observations provided spatiotemporal dynamics of alkyne SERS signals such as spatial movements and intensity blinking, suggests that the precise co-localization between any given gold nanoparticles and drug molecules can rapidly change at the single nanoparticle level. The advantage of this technique, however, is that we can measure multiple SERS signals at multiple time points from multiple cells without needing to resolve the precise co-localization of both nanoparticles and drug molecules and can visualize overall drug uptake over time (as results in Figure 4 show). Using other optical imaging techniques in combination with measuring SERS spectra may provide additional utility. As one approach, combining the current system with nanoparticle-tracking system by dark-field imaging would enable to obtain SERS spectra with

higher spatial and temporal resolution, and this might provide a way to improve detection of drug molecules and interactions with the local chemical environment using functionalized nanoparticles.[51]

We proposed quantitative analysis using digital SERS counting to statistically visualize the temporal behaviors of the number of SERS spots of alkyne. This digital SERS counting was originally proposed to quantify analytes at low concentrations at the single-molecule level.[43] In our experiments, we could not ensure that the SERS signals in the cells were from single molecules; therefore, the number of SERS spots could not be used to obtain an absolute number of molecules. We therefore utilized the digital SERS counting method to monitor the relative change of drug concentrations, and especially the evolution of drug uptake over time, under different physical and chemical environments.

SERS detections of various alkyne-tagged molecules have recently been demonstrated using different biological models such as H9c2 cells,[27] NIH-3T3 cells,.[28] and MCF-7 cells.[29] We then expect our technique is applicable across other cell lines and small molecule drugs. One challenge for the type of dynamic studies we propose here is that the degree of uptake of nanoparticles does vary with the cell types. However, even in cell types where uptake is less frequent, methods have been developed to improve both nanoparticle uptake rate and localization, which are needed to sensitively detect drug delivery and specify locations. Using surface modifications with signal peptides[52] would be useful to introduce nanoparticle to monitor the entry of tagged molecules into a nucleus. Passive uptake of nanoparticles can also be achieved using electroporation[53] to introduce the nanoparticles to cytoplasm through a cell membrane.

The temporal resolution can be improved by boosting SERS signal of alkynes with plasmon-enhanced SRS (PESRS) process. Recently developed PESRS microscopy[54,55] can be a promising technique toward ultra-fast imaging of spatiotemporal dynamics of small molecules drugs in live cells with single-molecule sensitivity.

METHODS

Slit-scanning Raman microscopy. See Figure S2 for the schematic of our microscopy setup. A home-built slit-scanning Raman microscope was used for Raman and SERS spectroscopy and imaging. A solid-state laser with a wavelength of 660 nm (opus660, Laser Quantum) was used for SERS measurement, and a solid-state laser with a wavelength of 532 nm (Millennia eV, Spectra Physics) was used for the Raman spectroscopy. Cylindrical lenses were used to create line-shaped laser light at the focal plane. The laser was focused on the sample through a water-immersion objective lens (Apo, 1.25 N.A., 40×, Nikon or Plan Apo IR, 1.27 N.A., 60×, Nikon) mounted to an inverted microscope (ECLIPSE Ti, Nikon). Light scattered in the sample was collected by the same objective. Rayleigh scattering was blocked by long pass filters (LP02-664RU-25 for 660 nm, LP03-532RU-25 for 532 nm excitations, Semrock) and Raman scattered light was focused on an entrance slit with a width of 50 μm of an imaging polychromator (MK-300, Bunko Keiki) through a tube lens. The Raman spectra were then detected with a cooled EM-CCD camera (iXon Ultra888, Andor). A galvano-meter mirror was used for scanning the line in the x-direction. A piezoelectric translation stage was used for scanning the line in the z-direction for 3D SERS imaging.

Spontaneous Raman spectroscopy of Alt-AOMK. Spontaneous Raman spectra of Alt-AOMK were collected with a home-built Raman microscope equipped with a 532 nm excitation laser and

a 60× objective lens to effectively obtain Raman scattered light from the sample. A total of 2 μL of Alt-AOMK at each concentration dissolved in DMSO (Figure 1B, Figure S1) were placed on glass bottom dishes with a diameter of 35 mm (Matsunami). The laser intensity at the sample was 2 mW/μm^2. The exposure time was 20 s. A total of 200 Raman spectra were simultaneously collected and the averaged spectrum was used as a resultant Raman spectrum of the sample.

SERS spectroscopy of Alt-AOMK with gold nanoparticles on glass substrate. Gold nanoparticles with a diameter of 50 nm (EMGC50, BBI solutions) was used for the SERS measurements. The mean size of the particles was from 47 nm to 53 nm with coefficient of variance of less than 8%. The peak position of the extinction spectrum of gold nanoparticle suspension, measured with UV-Vis spectroscopy (Multiskan GO, Thermo Fisher Scientific), was at 535 nm (Figure S12). A MAS-coated cover glass with a diameter of 25 mm (Matsunami) was used as the substrate. A 2 μL of the gold nanoparticle suspension was dropped on the glass substrate and dried for 60 min. The negative charge of the citric acids at the surface of the gold nanoparticles strongly conjugated with an amino group on the glass substrate and a monolayer of aggregated gold nanoparticles was created. The gold nanoparticle-modified glass substrate was washed with distilled deionized water to remove extra gold nanoparticles. After drying with N_2 gas, 1 μL of Alt-AOMK at a concentration of 10 μM was dropped onto the substrate. SERS measurement of the sample was performed with a home-built Raman microscope equipped with a 660 nm excitation laser and a 60× objective lens. The laser intensity at the sample plane was 0.79 mW/μm^2. The exposure time per line was 50 ms. One of the representative SERS spectra of Alt-AOMK is shown in Figure 1B.

Introducing gold nanoparticles into live cells. Macrophages (J774A.1) were cultured in glass bottom dishes with a density of 2–3 × 10^5 cells/mL with DMEM (043-30058, FUJIFILM Wako

Pure Chemical Corporation) supplemented with fetal bovine serum (SH30071.03, GE Healthcare HyClone) and penicillin-streptomycin (26252-94, Nacalai Tesque) as an antibiotic. Cells were maintained in an incubator (Sanyo) of 37 °C and 5% CO_2 environment for 6 h. The cells were washed several times with phosphate buffered saline (PBS). The cells were again incubated with DMEM containing 100 μL of gold nanoparticle suspension with a diameter of 50 nm (EMGC50, BBI solutions) with a density of 2.25×10^9 particles/mL for 16 h. During the incubation for 16 h, gold nanoparticles have been shown to be delivered to lysosomes through endocytosis and to form aggregates of several nanoparticles.[46] The diameter of 50 nm is an optimal size for live cells to uptake them through endocytosis.[56] After the incubation with the gold nanoparticles, the cells were washed again several times with PBS to remove the gold nanoparticles outside the cells. The cells were filled again with DMEM and stored in the incubator.

Raman imaging of Alt-AOMK in live cells with and without gold nanoparticles. Macrophages were cultured with and without gold nanoparticles in glass bottom dishes. The two samples were filled with DMEM containing Alt-AOMK at a concentration of 10 μM and incubated for 2 h at 37 °C and 5% CO_2. The two samples were then measured with a home-built Raman microscope equipped with a 60× objective lens. We used 660 nm excitation laser for live-cell SERS imaging. Although the wavelength is slightly far from the resonance wavelength at 535 nm for the gold nanoparticles, we still obtained high enhancement and the longer excitation wavelength can reduce phototoxicity to the cells and scattering from the nanoparticles, and allow us to observe time-series of SERS dataset. The laser intensity at the sample plane was 0.63 mW/μm^2. The exposure time per line was 50 ms. One Raman image was acquired from 100 scanning lines in the x-direction (Figure S3).

Time-lapse 2D SERS imaging of live cells. Macrophages were cultured with gold nanoparticles in two glass bottom dishes. One of the dishes was filled with 2 mL of DMEM containing Alt-AOMK at a concentration of 10 μM for 4 h at 37 °C and 5% CO_2 (Figure 2, Supporting Movie 1). The other dish was filled with 2 mL of DMEM without Alt-AOMK for 4 h at 37 °C and 5% CO_2 (Supporting Movie 2). The two samples were measured using a home-built Raman microscope equipped with a 660 nm excitation laser and a 40× objective lens. The laser intensity of the sample plane was 1.3 mW/μm^2. The exposure time per line was 50 ms. One Raman image was acquired from 120 scanning steps in the x-direction with an acquisition time of 6.5 s. A total of 400 Raman images were obtained in approximately 43 min.

3D SERS imaging of live cells with Alt-AOMK. Macrophages were cultured with gold nanoparticles in glass bottom dishes. Alt-AOMK was added to the cell culturing medium at a concentration of 5 μM. After 30 min, the cells were measured using a home-built 3D Raman microscope equipped with a 660 nm excitation laser and a 60× objective lens. The laser intensity of the sample plane was 0.78 mW/μm^2. The exposure time per line was 50 ms. A 3D SERS image was acquired with 40 and 10 scanning steps in the x- and z-directions, respectively, with an acquisition time of 21.8 s (Figure S5).

Time-lapse 3D SERS imaging of live cells with Alt-AOMK. Macrophages were cultured with gold nanoparticles in glass bottom dishes. Cells were measured by a home-built 3D Raman microscope equipped with a 660 nm excitation laser and a 60× objective lens. The laser intensity of the sample plane was 0.78 mW/μm^2. The exposure time per line was 50 ms. A 3D Raman image was acquired from 40 scanning steps in the x-direction and 10 scanning steps in the z-direction. The acquisition time was 21.8 s. A total of 150 Raman images were obtained in approximately 53 min. In the middle of the measurement (at the 20th frame), Alt-AOMK was gently introduced into

the cell culturing medium at final concentrations of 0, 1, 20, 50, and 100 μM for each sample (Figure 3, Figure 4, Figure S9, Supporting Movie 3, and Supporting Movie 4). The SERS imaging was performed 2–3 times at each concentration to increase the number of cells. Bright field images of the cells before and after the SERS measurement were recorded with a sCMOS camera (Zyla 4.2, Andor) attached to the side port of the microscope (Figure S6, Figure S7). For the time-lapse 3D SERS imaging of the cells under endocytosis inhibition (Figure S11, Supporting Movie 5), macrophages with gold nanoparticles were placed in a fridge at 4 °C for 90 min. The cells were then measured under the same imaging conditions as described above. The administration concentration of Alt-AOMK in the cell culturing medium was 5 μM. As a comparison, macrophages incubated at 37 °C (normal condition) were measured under the same concentration (Figure S11, Supporting Movie 5).

3D SERS imaging of live cells at 37 °C and 4 °C. Macrophages were cultured in two glass bottom dishes. One of the dishes was incubated with gold nanoparticles with a density of 2.25×10^9 particles/mL for 2 h at 37 °C, and the other was incubated with gold nanoparticles with the same particle density for 2 h at 4 °C (Figure S10). Then, the two samples were washed with PBS to remove the gold nanoparticles outside the cells. The samples were filled again with 2 mL of DMEM. The two samples were measured with a home-built 3D Raman microscope equipped with a 660 nm excitation laser and a 60× objective. The laser intensity at the sample plane was 2.62 mW/μm^2. The exposure time per line was 50 ms. One 3D SERS image was acquired from 40 scanning steps in the x-direction and 10 scanning steps in the z-direction. The images were recorded with an acquisition time of 21.8 s. The z-projected 2D SERS images are shown in Figure S10.

Cell viability assay. Macrophages with and without gold nanoparticles were prepared with the same procedure above. For the macrophages with gold nanoparticles, Alt-AOMK was introduced at 0 μM, 20 μM, and 100 μM for each sample, and the cells were incubated again at 37 °C. After trypsinization, centrifugation was performed to collect the cells. Each cell sample was diluted by 2 times with 0.4% Trypan Blue solution (Thermo Fisher Scientific). 10 μL of the diluted cell sample was then carefully introduced into a disposable hemocytometer (NanoEnTek). Dead and live cells were counted under the bright field microscope for four 1 x 1 mm squares (Figure S4).

Data and statistical analysis. After Raman imaging, all Raman hyperspectral datasets were processed using home-written program with MATLAB (MathWorks). The color of Raman images was assigned by ImageJ. The 3D Raman images were created by Volume Viewer in ImageJ. Statistical analysis was performed using MATLAB and Igor Pro (WaveMetrics). The values for N and the specific statistical processing for each experiment are described in the figure legend, in the figure caption, or in the main text.

ASSOCIATED CONTENT

Supporting Information (file type, PDF): Detection limit of spontaneous Raman peak of alkyne in Alt-AOMK (Figure S1); Optical setup of a slit-scanning SERS microscope (Figure S2); Raman imaging of live macrophages with and without gold nanoparticles (Figure S3); Bright field observation of macrophages with hemocytometers for cell viability assay using trypan blue solution (Figure S4); 3D SERS imaging of live macrophages with Alt-AOMK (Figure S5); Bright field observation of live macrophages before and after the time-lalpse 3D SERS measurement (Figure S6); Bright field observation of live macrophages before and after the time-lapse 3D SERS

measurement at concentrations of 20 μM with laser irradiation (A) and without laser irradiation (B) (Figure S7); Processing flow for the alkyne peak detection (Figure S8); Digital SERS counting of Alt-AOMK in each cell (Figure S9); 3D SERS imaging of live macrophages with gold nanoparticles incubated at 37 °C and 4 °C (Figure S10); Temporal behaviors of the number of SERS spots of live macrophages incubated at 37 °C (red plot) and 4 °C (blue plot) (Figure S11); UV-Vis spectrum of gold nanoparticles with diameter of 50 nm (Figure S12); Summary of cell viability assay for investigating nanoparticles and drug toxicity for live cells (Table S1)

Supporting Movie 1 (file type, mov): Time-lapse 2D SERS imaging of live cells with gold nanoparticles and Alt-AOMK.

Supporting Movie 2 (file type, mov): Time-lapse 2D SERS imaging of live cells with gold nanoparticles and without Alt-AOMK.

Supporting Movie 3 (file type, mov): Time-lapse 3D SERS imaging of live cells with Alt-AOMK.

Supporting Movie 4 (file type, mov): Time-lapse 3D SERS imaging of live cells at different administration concentrations of Alt-AOMK.

Supporting Movie 5 (file type, mov): Time-lapse 3D SERS imaging of live cells incubated at 37 °C and 4 °C.

The Supporting Information and Supporting Movies are available free of charge on the ACS Publication website at http://pubs.acs.org.

The authors declare no conflict of financial interest.

AUTHOR INFORMATION

Corresponding Author

*Katsumasa Fujita

Department of Applied Physics, Osaka University, 2-1 Yamadaoka, Suita, Osaka 565-0871, Japan.

Email: fujita@ap.eng.osaka-u.ac.jp

Present Addresses

Jun Ando: Molecular Physiology Laboratory, RIKEN, 2-1 Hirosawa, Wako, Saitama 351-0198, Japan.

Hiroyuki Yamakoshi: Graduate School of Pharmaceutical Sciences, Tohoku University, 6-3 Aza-Aoba, Aramaki, Aoba-ku, Sendai, Miyagi 980-8578, Japan

ORCID

Kota Koike: 0000-0002-5631-5138

Jun Ando: 0000-0003-1677-8426

Naoki Terayama: 0000-0002-4025-8060

Kosuke Dodo: 0000-0001-6008-2915

Mikiko Sodeoka: 000-0002-1344-364X

Author Contributions

† These authors contributed equally to this work.

K.F., N.S., and M.S. conceived the concept; K.K., K.B., J.A, and K.F. designed and performed the experiments; K.K. and K.B. analyzed the data; H.Y., K.D., and M.S. contributed the design of chemical compounds; N.T. and H.Y. synthesized the chemical compounds; K.K., K.B., and K.F. wrote the manuscript with input from J.A, H.Y., K.D., N.S., and M.S.

Acknowledgements

This research was supported by AMED-CREST and JSPS KAKENHI under Grant Numbers JP18gm071000 and 26000011, respectively.

REFERENCES

1. Puppels, G. J.; de Mul, F. F.; Otto, C.; Greve, J.; Robert-Nicoud, M.; Arndt-Jovin, D. J.; Jovin, T. M. Studying Single Living Cells and Chromosomes by Confocal Raman Microspectroscopy. *Nature* **1990**, *347*, 301–303.

2. van Manen, H.-J.; Kraan, Y. M.; Roos, D.; Otto, C. Intracellular Chemical Imaging of Heme-Containing Enzymes Involved in Innate Immunity Using Resonance Raman Microscopy. *J. Phys. Chem. B* **2004**, *108*, 18762–18771.

3. Hamada, K.; Fujita, K.; Smith, N. I.; Kobayashi, M.; Inouye, Y.; Kawata, S. Raman Microscopy for Dynamic Molecular Imaging of Living Cells. *J. Biomed. Opt.* **2008**, *13*, 044027.

4. Okada, M.; Smith, N. I.; Palonpon, A. F.; Endo, H.; Kawata, S.; Sodeoka, M.; Fujita, K. Label-Free Raman Observation of Cytochrome c Dynamics during Apoptosis. *Proc. Natl. Acad. Sci. U. S. A.* **2012**, *109*, 28–32.

5. Massoud, T. F.; Gambhir, S. S. Molecular Imaging in Living Subjects: Seeing Fundamental Biological Processes in a New Light. *Genes Dev*. **2003**, *17*, 545–580.

6. Willmann, J. K.; van Bruggen, N.; Dinkelborg, L. M.; Gambhir, S. S. Molecular Imaging in Drug Development. *Nat. Rev. Drug Discov.* **2008**, *7*, 591–607.

7. Yamakoshi, H.; Dodo, K.; Okada, M.; Ando, J.; Palonpon, A.; Fujita, K.; Kawata, S.; Sodeoka, M. Imaging of EdU, an Alkyne-Tagged Cell Proliferation Probe, by Raman Microscopy. *J. Am. Chem. Soc.* **2011**, *133*, 6102–6105.

8. Yamakoshi, H.; Dodo, K.; Palonpon, A.; Ando, J.; Fujita, K.; Kawata, S.; Sodeoka, M. Alkyne-Tag Raman Imaging for Visualization of Mobile Small Molecules in Live Cells. *J. Am. Chem. Soc.* **2012**, *134*, 20681–20689.

9. Best, M. D. Click Chemistry and Bioorthogonal Reactions: Unprecedented Selectivity in the Labeling of Biological Molecules. *Biochemistry* **2009**, *48*, 6571–6584.

10. Cañeque, T.; Müller, S.; Rodriguez, R. Visualizing Biologically Active Small Molecules in Cells Using Click Chemistry. *Nat. Rev. Chem.* **2015**, *2*, 202–215.

11. Ando, J.; Kinoshita, M.; Cui, J.; Yamakoshi, H.; Dodo, K.; Fujita, K.; Murata, M.; Sodeoka, M. Sphingomyelin Distribution in Lipid Rafts of Artificial Monolayer Membranes Visualized by Raman Microscopy. *Proc. Natl. Acad. Sci. U. S. A.* **2015**, *112*, 4558–4563.

12. Yamakoshi, H.; Palonpon, A.; Dodo, K.; Ando, J.; Kawata, S.; Fujita, K.; Sodeoka, M. A Sensitive and Specific Raman Probe Based on Bisarylbutadiyne for Live Cell Imaging of Mitochondria. *Bioorg. Med. Chem. Lett.* **2015**, *25*, 664–667.

13. El-Mashtoly, S. F.; Petersen, D.; Yosef, H. K.; Mosig, A.; Reinacher-Schick, A.; Kötting, C.; Gerwert, K. Label-Free Imaging of Drug Distribution and Metabolism in Colon Cancer Cells by Raman Microscopy. *Analyst* **2014**, *139*, 1155–1161.

14. Wei, L.; Hu, F.; Shen, Y.; Chen, Z.; Yu, Y.; Lin, C. C.; Wang, M. C.; Min, W. Live-Cell Imaging of Alkyne-Tagged Small Biomolecules by Stimulated Raman Scattering. *Nat. Methods* **2014**, *11*, 410–412.

15. Fu, D.; Zhou, J.; Zhu, W. S.; Manley, P. W.; Wang, Y. K.; Hood, T.; Wylie, A.; Xie, X. S. Imaging the Intracellular Distribution of Tyrosine Kinase Inhibitors in Living Cells with Quantitative Hyperspectral Stimulated Raman Scattering. *Nat. Chem.* **2014**, *6*, 614–622.

16. Sepp, K.; Lee M.; Bluntzer, M. T. J.; Helgason, G. V.; Hulme, A. N.; Brunton, V. G. Utilizing Stimulated Raman Scattering Microscopy to Study Intracellular Distribution of Label-Free Ponatinib in Live Cells. *J. Med. Chem*. **2020**, *63*, 2028–2034.

17. Hu, F.; Zeng, C.; Long, R.; Miao, Y.; Wei, L.; Xu, Q.; Min, W. Supermultiplexed Optical Imaging and Barcoding with Engineered Polyynes. *Nat. Methods* **2018**, *15*, 194–200.

18. Tipping, W. J.; Lee, M; Serrels, A.; Brunton, V. G.; Hulme, A. N. Imaging Drug Uptake by Bioorthogonal Stimulated Raman Scattering Microscopy. *Chem. Sci.* **2017**, *8*, 5606-5615.

19. Kneipp, K.; Wang, Y.; Kneipp, H.; Perelman, L. T.; Itzkan, I.; Dasari, R. R.; Feld, M. S. Single Molecule Detection Using Surface-Enhanced Raman Scattering (SERS). *Phys. Rev. Lett.* **1997**, *78*, 1667–1670.

20. Pieczonka, N. P. W.; Aroca, R. F. Single Molecule Analysis by Surfaced-Enhanced Raman Scattering. *Chem. Soc. Rev.* **2008**, *37*, 946–954.

21. Le Ru, E. C.; Etchegoin, P. G. Single-Molecule Surface-Enhanced Raman Spectroscopy. *Annu. Rev. Phys. Chem.* **2012**, *63*, 65–87.

22. Shiota, M.; Naya, M.; Yamamoto, T.; Hishiki, T.; Tani T.; Takahashi, H.; Kubo, A.; Koike, D.; Itoh, M.; Ohmura, M.; Kabe, Y; Sugiura, Y; Hiraoka, N; Morikawa, T; Takubo, K; Suina, K; Nagashima, H; Sampetrean O; Nagano, O; Saya, H. *et al*. Gold-Nanofève Surface-Enhanced Raman Spectroscopy Visualizes Hypotaurine as a Robust Anti-Oxidant Consumed in Cancer Survival. *Nat. Commun*. **2018**, *9*, 1561.

23. Kneipp, K.; Haka, A. S.; Kneipp, H., Badizadegan, K.; Yoshizawa, N.; Boone, C.; Shafer-Peltier, K. E.; Motz, J. T.; Dasari, R. R.; Feld, M. S. Surface-Enhanced Raman Spectroscopy in Single Living Cells Using Gold Nanoparticles. *Applied Spectroscopy* **2002**, *56*, 150–154.

24. Kneipp, J.; Kneipp, H.; McLaughlin, M.; Brown, D.; Kneipp, K. In Vivo Molecular Probing of Cellular Compartments with Gold Nanoparticles and Nanoaggregates. *Nano Lett*. **2006**, *6*, 2225–2231.

25. Fujita, K.; Ishitobi, S.; Hamada, K.; Smith, N. I.; Taguchi, A.; Inouye, Y.; Kawata, S. Time-Resolved Observation of Surface-Enhanced Raman Scattering from Gold Nanoparticles during Transport through a Living Cell. *J. Biomed. Opt*. **2009**, *14*, 024038.

26. Ando, J.; Fujita, K.; Smith, N. I.; Kawata, S. Dynamic SERS Imaging of Cellular Transport Pathways with Endocytosed Gold Nanoparticles. *Nano Lett*. **2011**, *11*, 5344–5348.

27. Kennedy, D. C.; Hoop, K. A.; Tay, L.-L.; Pezacki, J. P. Development of Nanoparticle Probes for Multiplex SERS Imaging of Cell Surface Proteins. *Nanoscale* **2010**, *2*, 1413–1416.

28. Ardini, M.; Huang, J.-A.; Sánchez, C. S.; Mousavi, M. Z.; Caprettini, V.; Maccaferri, N.; Melle, G.; Bruno, G.; Pasquale, L.; Garoli, D.; Angelis, F. D. Live Intracellular Biorthogonal Imaging by Surface Enhanced Raman Spectroscopy Using Alkyne- Silver Nanoparticles Clusters. *Sci. Rep.* **2018**, *8*, 12652.

29. Li, M.; Wu, J.; Ma, M.; Feng, Z.; Mi, Z.; Rong, P.; Liu, D. Alkyne- and Nitrile-Anchored Gold Nanoparticles for Multiplex SERS Imaging of Biomarkers in Cancer Cells and Tissues. *Nanotheranostics* **2019**, *3*, 113–119.

30. Tanuma, M.; Kasai, A.; Bando, K.; Kotoku, N.; Harada, K.; Minoshima, M.; Higashino, K.; Kimishima, A.; Arai, M.; Ago, Y.; Seiriki, K; Kikuchi, K; Kawata, S; Fujita, K; Hashimoto, H. Direct Visualization of an Antidepressant Analog Using Surface-Enhanced Raman Scattering in the Brain. *JCI Insight* **2020**, *5*, e133348.

31. Huefner, A.; Kuan, W.-L.; Müller, K. H.; Skepper, J. N.; Barker, R. A.; Mahajan, S. Characterization and Visualization of Vesicles in the Endo-Lysosomal Pathway with Surface-Enhanced Raman Spectroscopy and Chemometrics. *ACS Nano* **2016**, *10*, 307–316.

32. Long, N. J.; Williams, C. K. Metal Alkynyl σ Complexes: Synthesis and Materials. *Angew. Chem. Int. Ed.* **2003**, *42*, 2586–2617.

33. Ando, J.; Asanuma, M.; Dodo, K.; Yamakoshi, H.; Kawata, S.; Fujita, K.; Sodeoka, M. Alkyne-Tag SERS Screening and Identification of Small-Molecule-Binding Sites in Protein. *J. Am. Chem. Soc.* **2016**, *138*, 13901–13910.

34. Kato, D.; Boatright, K. M.; Berger, A. B.; Nazif, T.; Blum, G.; Ryan, C.; Chehade, K. A. H.; Salvesen, G. S.; Bogyo, M. Activity-Based Probes that Target Diverse Cysteine Protease Families. *Nat. Chem. Biol.* **2005**, *1*, 33–38.

35. Patterson, M. L.; Weaver, M. J. Surface-Enhanced Raman Spectroscopy as a Probe of Adsorbate-Surface Bonding: Simple Alkenes and Alkynes Adsorbed at Gold Electrodes. *J. Phys. Chem.* **1985**, *89*, 5046–5051.

36. Manzel, K.; Schulze, W.; Moskvits, M. Surface-Enhanced Raman Spectra of C_2H_2 and C_2H_4 Adsorbed on Silver Colloid. *Chem. Phys. Lett.* **1982**, *85*, 183–186.

37. Feilchenfeld, H.; Weaver, M. J. Binding of Alkynes to Silver, Gold, and Underpotential Deposited Silver Electrodes as Deduced by Surface-Enhanced Raman Spectroscopy. *J. Phys. Chem.* **1989**, *93*, 4276–4282.

38. Joo, S.-W.; Kim, K. Adsorption of Phenylacetylene on Gold Nanoparticle Surfaces Investigated by Surface-Enhanced Raman Scattering. *J. Raman. Spectrosc.* **2004**, *35*, 549–554.

39. Lutgens, S. P. M.; Cleutjens, K. B. J. M.; Daemen, M. J. A. P.; Heeneman, S. Cathepsin Cysteine Proteases in Cardiovascular Disease. *FASEB J.* **2007**, *21*, 3029–3041.

40. Mizunoe, Y.; Kobayashi, M.; Hoshino, S.; Tagawa, R.; Itagawa, R.; Hoshino, A.; Okita, N.; Sudo, Y.; Nakagawa, Y.; Shimano, H.; Higami, Y. Cathepsin B Overexpression Induces Degradation of Perilipin 1 to Cause Lipid Metabolism Dysfunction in Adipocytes. *Sci. Rep.* **2020**, *10*, 634.

41. Ha, S.-D.; Martins, A.; Khazaie, K.; Han, J; Chan, M. C. B.; Kim, S. O. Cathepsin B Is Involved in the Trafficking of TNF-α-Containing Vesicles to the Plasma Membrane in Macrophages. *J. Immunol.* **2008**, *181*, 690–697.

42. Palonpon, A. F.; Ando, J.; Yamakoshi, H.; Dodo, K.; Sodeoka, M.; Kawata, S.; Fujita, K. Raman and SERS Microscopy for Molecular Imaging of Live Cells. *Nat. Protoc.* **2013**, *8*, 677-692.

43. Etchegoin, P. G.; Le Ru, E. C. Resolving Single Molecules in Surface-Enhanced Raman Scattering within the Inhomogeneous Broadening of Raman Peaks. *Anal. Chem.* **2010**, *82*, 2888–2892.

44. Marshall, A. R. L.; Stokes, J.; Viscomi, F. N.; Proctor, J. E.; Gierschner, J.; Bouillard, J.-S. G.; Adawi, A. M. Determining Molecular Orientation *via* Single Molecule SERS in a Plasmonic Nano-Gap. *Nanoscale* **2017**, *9*, 17415-17421.

45. Lindquist, N. C.; de Albuquerque, C. D. L.; Sobral-Filho, R. G.; Paci, I.; Brolo, A. G. High-Speed Imaging of Surface-Enhanced Raman Scattering Fluctuations from Individual Nanoparticles. *Nat. Nanotechnol.* **2019**, *14*, 981–987.

46. Liu, M.; Li, Q.; Liang, L.; Li, J.; Wang, K.; Li, J.; Lv, M.; Chen, N.; Song, H.; Lee, J.; Shi, J.; Wang, L.; Lal, R.; Fan, C. Real-Time Visualization of Clustering and Intracellular Transport of Gold Nanoparticles by Correlative Imaging. *Nat. Commun.* **2018**, *8*, 15646.

47. de Albuquerque, C. D. L.; Sobral-Filho, R. G.; Poppi, R. J.; Brolo, A. G. Digital Protocol for Chemical Analysis at Ultralow Concentrations by Surface-Enhanced Raman Scattering. *Anal. Chem.* **2018**, *90*, 1248–1254.

48. Zhang, Y.; Noji, H. Digital Bioassays: Theory, Applications, and Perspectives. *Anal. Chem.* **2017**, *89*, 92–101.

49. Tomoda, H.; Kishimoto, Y.; Lee, Y. C. Temperature Effect on Endocytosis and Exocytosis by Rabbit Alveolar Macrophages. *J. Biol. Chem.* **1989**, *264*, 15445–15450.

50. Punnonen, E.-L.; Ryhanen, K.; Marjomaki, V. S. At Reduced Temperature, Endocytic Membrane Traffic Is Blocked in Multivesicular Carrier Endosomes in Rat Cardiac Myocytes. *Eur. J. Cell Biol.* **1997**, *75*, 344–352.

51. Bando, K.; Zhang, Z.; Graham, D.; Faulds, K.; Fujita, K.; Kawata, S. Dynamic pH Measurements of Intracellular Pathways Using Nano-Plasmonic Assemblies. *Analyst* **2020**, *145*, 5768–5775.

52. Huefner, A.; Kuan, W.-L.; Barker, R. A.; Mahajan, S. Intracellular SERS Nanoprobes for Distinction of Different Neuronal Cell Types. *Nano Lett.* **2013**, *13*, 2463–2470.

53. Lin, J.; Chen, R.; Feng, S.; Li, Y.; Huang, Z.; Xie, S.; Yu, Y.; Cheng, M.; Zeng, H. Rapid Delivery of Silver Nanoparticles into Living Cells by Electroporation for Surface-Enhanced Raman Spectroscopy. *Biosens. Bioelectron.* **2009**, *25*, 388–394.

54. Frontiera, R. R.; Henry, A.-I.; Gruenke, N. L.; Van Duyne, R. P. Surface-Enhanced Femtosecond Stimulated Raman Spectroscopy. *J. Phys. Chem. Lett.* **2011**, *2*, 1199–1203.

55. Zong, C.; Premasiri, R.; Lin, H.; Huang, Y.; Zhang, C.; Yang, C.; Ren, B.; Ziegler, L. D.; Cheng, J.-X. Plasmon-Enhanced Stimulated Raman Scattering Microscopy with Single-Molecule Detection Sensitivity. *Nat. Commun.* **2019**, *10*, 5318.

56. Chithrani, B. D.; Ghazani, A. A.; Chan, W. C. W. Determining the Size and Shape Dependence of Gold Nanoparticle Uptake into Mammalian Cells. *Nano Lett.* **2006**, *6*, 662–668.

Table of Contents graphic